Bulletin of the Seismological Society of America, Vol. 100, No. 5B, pp. 2791–2804, November 2010, doi: 10.1785/0120090244

The 12 May 2008 M_w 7.9 Wenchuan, China, Earthquake: Macroseismic Intensity Assessment Using the EMS-98 and ESI 2007 Scales and Their Correlation with the Geological Structure

by Efthymis L. Lekkas

Abstract The Wenchuan earthquake of 12 May 2008 in Sichuan Province, China, can be classified as a large-scale event based on the tectonic structures that triggered the earthquake and the effects caused on the human, structural, and natural environment.

This paper presents the geotectonic and seismotectonic regime of the earthquake-affected region on the basis of field data obtained along the seismic fault zone and provides: (1) an estimation of the intensity values according to the EMS-98 and the ESI 2007 scales and the determination of their large-scale geographical distribution along the causative tectonic structure, (2) an interpretation of the intensity distribution according to the seismotectonic, geodynamic, and geotechnical framework, and (3) a comparison between two different intensity scales, the EMS-98 (which is essentially based on the effects on the built environment) and the ESI 2007 (which is based on earthquake environmental effects). The application of both EMS-98 and ESI 2007 and the comparative review and evaluation of the results indicate that the estimated values of the EMS-98 and the ESI 2007 were similar. This suggests that both scales can be useful and reliable tools for seismic hazard estimation.

Introduction

On 12 May 2008, a great earthquake of M_w 7.9 struck south China. This catastrophic event caused extensive casualties and heavy engineering damage in a wide area along the Longmen Shan thrust belt. Numerous buildings collapsed or were damaged to various levels because of the fault displacement extending over 220 km and the abundance of earthquake-related phenomena, such as landslides, rockfalls, mudslides, and liquefaction. Basic lifeline systems such as transportation, electricity, communications, water supply and drainage, and gas and hydraulic structures were heavily damaged at a level not previously encountered in recent Chinese history. The heavily damaged roads, bridges, power lines, and other systems significantly obstacolated the earthquake relief activities, thus adding to the human and economic loss. Future large earthquakes will have a progressively increasing impact on the society, both in China and the rest of the world, due to the increasing expansion of densely populated areas in the past decades, as already illustrated vividly by the 2004 Sumatra earthquake.

As reported by the Chinese Ministry of Civil Affairs (4 September 2008), the death toll reached 69,226, and the number of missing was 17,923. Moreover, 374,200 injuries were recorded, and the number of homeless amounted to over 15 million. In some destroyed counties, such as Beichuan, homeless people exceeded 90% of the population. The estimated direct economic property loss (including infrastructure) is about 845 billion Renminbi (RMB, or $124 billion U.S.).

The epicenter of the earthquake was located in Yingxiu town (31.0° N, 103.4° E) in the southwest part of Wenchuan County, with a focal depth of 14 km according to China Earthquake Administration (CEA), 21 km from Dujiangyan and 75 km from the capital of Sichuan Province, Chengdu (Fig. 1).

The Wenchuan earthquake was the greatest earthquake to strike Sichuan province since the 1972 M_s 7.2 Songpan-Pingwu earthquake, and it was the most devastating in China since the 1976 Tangshan earthquake.

The aims of this paper are:

1. To briefly present the geotectonic and seismotectonic regime of the region affected by the earthquake based on field data along the causative fault.
2. To estimate the intensity values above intensity VI EMS-98/ESI 2007 according to the European Macroseismic Scale (EMS-98; Grünthal, 1998) and the Environmental Seismic Intensity (ESI 2007) scale (Michetti *et al.*, 2007) and to determine the large-scale spatial distribution along the causative tectonic structure.

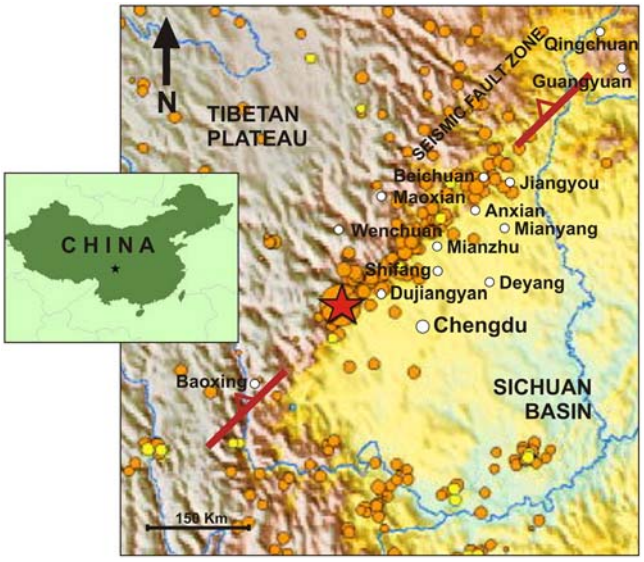

Figure 1. Generalized geographical map of the affected region with the epicenter location (star, USGS, 2008) and the seismic zone location (bold line). The color version of this figure is available only in the electronic edition.

3. To interpret the intensity values data and their distribution according to the seismotectonic, geodynamic, and geotechnical regime.
4. To conduct a comparative review and evaluation on the application of both the EMS-98 and the ESI 2007 scales.

Geodynamic–Seismotectonic Framework

The focus of the earthquake was located on the Longmen Shan thrust belt, which is a well-studied thrust fault zone in the northwest of Sichuan Province (Burchfiel *et al.*, 2008; Chen *et al.*, 2008). This thrust belt starts from Luding and Tianquan in the south (located outside the map area shown in Fig. 1), extends north-eastwards through Baoxing, Dujiangyan (Guanxian), Beichuan, Jiangyou, and Guangyuan (Fig. 1), up to Mianxian of Shanxi Province (located outside the map area shown in Fig. 1). The total length is about 500 km, the width is 40–50 km, and the general strike is northeast–southwest.

The thrust belt comprises three splays, the front-range fault, the central fault, and the back-range fault (Fig 2 and Fig. 3). The southern segments of these fault splays are the Guanxian–Anxian fault, Yingxiu–Beichuan fault, and Wenchuan–Maoxian fault, respectively (Fig. 2 and Fig. 3)

The earthquake generated 220 km of surface rupture along the Yingxiu–Beichuan fault (Fig. 4), characterized by right-lateral oblique slip, and 72 km of surface rupture along the Guanxian–Anxian fault, characterized by reverse slip. Maximum vertical and horizontal displacements of 6.2 m and 4.9 m, respectively, were recorded along the Yingxiu–Beichuan fault, whereas maximum vertical and horizontal displacements of 3.5 m and 1.0 m, respectively were recorded along the Guanxian–Anxian fault (Chen *et al.*, 2008; Hao *et al.*, 2008; Xu *et al.*, 2008).

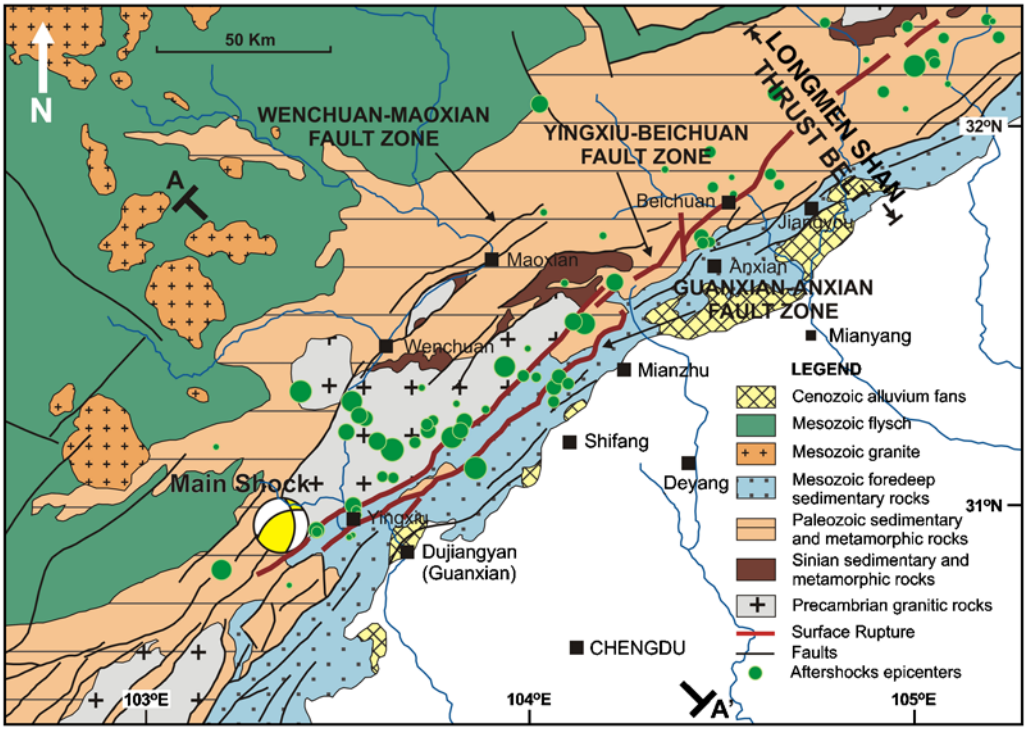

Figure 2. Geologic map of the greater earthquake-affected region (12 May 2008), exhibiting the activated faults, the main shock location, and the epicenters of the main aftershocks (modified, from Burchfiel *et al.*, 1995, Densmore *et al.*, 2007). The color version of this figure is available only in the electronic edition.

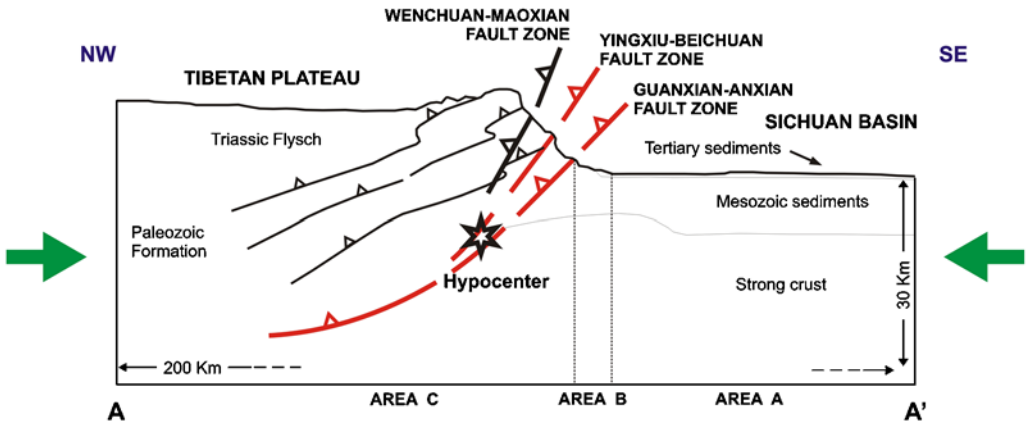

Figure 3. Geologic section trending northwest–southeast across the tectonic structure of the affected region with the activated faults and the hypocenter location. Areas A, B, and C are noted to exhibit variations of the intensity values. The color version of this figure is available only in the electronic edition.

Surficial faulting was observed along the rupture zone from the epicenter and for 220 km to the northeast. Further northeast, sporadic surficial faulting was also identified for a distance of 100 km.

According to an official announcement by the CEA, 260 aftershocks with magnitude greater than 4.0 had occurred by 15 August 2008, including 40 aftershocks that exceeded M_s 5.0 and 8 aftershocks that exceeded M_s 6.0, with the strongest one measuring M_s 6.4. The regional seismicity over the last two years prior to the main shock did not include any significant earthquake, with only two events of magnitude smaller than M_s 5.2.

Figure 4. The Yingxiu–Beichuan seismic fault at the outskirts of Yingxiu town. The color version of this figure is available only in the electronic edition.

According to the historical documents and the instrumental records, no earthquake exceeding M_s 6.0 had occurred in the north part of the Longmen Shan thrust belt. Instead, three M_s 6.0–6.5 strong earthquakes occurred in the middle and south parts of the Longmen Shan thrust belt: the M_s 6.5 Wenchuan earthquake on 21 April 1657, the M_s 6.4 Beichuan earthquake on 8 February 1958, and the M_s 6.3 Dayixi earthquake on 24 February 1958.

The overall strike of the fault zone is N45°E, with a 50–70° dip angle toward the northwest. This large-scale fault zone is not only the boundary between the Ganqing Block and the South China Block, but also forms the boundary between the mountainous area and the basin of Sichuan. In particular, it separates: (1) the extended region of the Tibetan Plateau toward the west—northwest with high altitudes exceeding 5000 m and (2) the lowlands of the Sichuan basin toward the southeast with altitudes not exceeding 1000 m. The Longmen Shan thrust belt formed in the Mesozoic. Since the Cenozoic, the collision between the Indian plate and the Eurasian plate has generated an intense compressional regime that causes regional deformation characterized by overthrusting nappes. The continuous uplift of the Longmen Shan, coupled with the depression of the piedmont has given rise to multiple denudation surfaces. In the Late Quaternary (Late Pleistocene to Holocene) the Longmen Shan thrust belt continues to be active; global positioning system measurements indicate that the east–west shortening rate of the fault belt is not significant (Lu *et al.*, 2003).

In conclusion, the distribution of this seismic fault, as well as its kinematics and dynamic characteristics, are attributed to the regional geodynamic setting, characterized by broad-scale thrusting of the Tibetan Plateau toward the east on the rigid block of the Sichuan basin. This is the result of

the prevailing compressional regime along the Himalayan Mountain belt, attributed to the progression of the Indian plate toward the north (Burchfiel *et al.*, 1995; Burchfiel, 2004; Zhang *et al.*, 2004; Densmore *et al.*, 2007; Gan *et al.*, 2007; Burchfiel *et al.*, 2008; Massachusetts Institute of Technology, 2008; Royden *et al.*, 2008; Tectonics Observatory of Caltech, 2008; U.S. Geological Survey (USGS), 2008; Hubbard and Shaw, 2009).

Intensity Estimation According to EMS-98

On the basis of field work and recordings of damage to infrastructure and constructions conducted in an extended region of the order of 50,000 km^2 and according to recent publications (Earthquake Engineering Research Institute (EERI), 2008; Houssam *et al.*, 2008; Hu *et al.*, 2008; Kabeyasawa *et al.*, 2008; Lekkas, 2008a; Li *et al.*, 2008; Sun *et al.*, 2008; Xu *et al.*, 2008), the following values and geographical distribution of intensities according to the EMS-98 (Grünthal, 1998) were observed.

Area A

Area A corresponds mainly to the extended lowland region of Sichuan Basin (Fig. 2 and Fig. 3) with altitudes not exceeding 1000 m.

A1. Shifang Region. The town of Shifang and the greater surrounding area are located on a morphologically flat region, approximately 20 km toward the southeast of the Guanxian–Anxian fault. It is estimated than 10% of the buildings collapsed or suffered severe damage, while more that 20% of the constructions underwent structural damage. These were multistory buildings, usually between two and six stories high, that probably experienced structural imperfections, while there was no systematic geographical differentiation of the collapses within the urban center. It should be pointed out that the foundation substratum corresponds to cohesive Quaternary formations, which unconformably lay on the rocky basement of the Sichuan basin and are not more than a couple of hundred meters thick. The estimated intensity value for this region is VI–VII$_{\text{EMS-98}}$.

A2. Mianyang Region. The Mianyang region is located on the morphologically lowland section 25–40 km toward the southeast of the fault trace. The recorded damage mainly includes fractures on the walls of first floors of modern constructions, while only a small number of multistory buildings collapsed or suffered serious structural damage. These were constructions up to six stories high that probably presented structural imperfections and did not follow the seismic design regulations. The geological—geotechnical conditions are uniform and are not differentiated from site to site within the urban center. In the greater area, cohesive Quaternary formations crop out, covering the older Sichuan basin formations.

The estimated intensity value for this area is on the order of VI–VII$_{\text{EMS-98}}$.

A3. Deyang Region. The town of Deyang and the surrounding area are located on the morphologically lowland section, approximately 40–60 km southeast of the seismic fault. The observed damage in the region includes mainly cracks on the walls of the first floors of modern constructions, while a small number of multistory buildings collapsed or suffered severe structural damage. Again, these five-story to six-story buildings most probably had structural imperfections and did not follow modern seismic design regulations. It should be mentioned that the distribution of damage in the urban area was random. The geological—geotechnical conditions are uniform all along the area and are similar to the two aforementioned ones.

The intensity value in this region is on the order of VI$_{\text{EMS-98}}$.

Area B

Essentially, area B is 10–20-km wide and 250-km long (Fig. 2 and Fig. 3) and corresponds to the elongated norhteast–southwest trending zone that includes the foothills of the Tibetan Plateau. More specifically, this area is bounded by the flat lowland region toward the southeast of the Sichuan basin and by the trace of the coseismic fault rupture to the northwest.

B1. Dujiangyan Region. The town of Dujiangyan is located 30 km east of the epicenter and 50 km west of the capital city Chengdu, in the zone defined by the boundary between the lowland and the high-relief regions and at a distance of only 5 km southeast of the seismic fault trace. The greatest part of the town is situated on a large alluvial fan formed by the Min River, which drains a wide mountainous region, while some of its branches run through the town. Moreover, the eastern, low-lying part of the town is founded on the Sichuan basin Quaternary formations, while its western part is founded on the Paleozoic and Mesozoic basement formations that form the foot of the mountainous region.

Within the town, approximately 300 constructions (approximately 5%) totally or partially collapsed, while 20% of the buildings suffered serious structural damage. Modern and older multistory reinforced concrete buildings were mainly the ones that collapsed. Most collapses were located on the foothills of the mountainous region toward the west and the morphologically higher areas; there were fewer in the lowlands. It is interesting to note that new buildings that were under construction and built to meet the modern seismic design regulations and were located toward the higher elevations of the town also collapsed or underwent serious structural damage. A crucial factor in these areas must have been the nature of the foundation formations, which comprise remnants of unconsolidated river deposits and debris of limited thickness on the rocky basement. It is estimated that 30%

of the building collapses observed in this town were located on similar deposits (Fig. 5 and Fig. 6).

Finally it should be emphasized that public buildings such as schools, hospitals, factories, and industrial constructions collapsed in the greater urban area.

The estimated general intensity value in the area is on the order of $VIII_{EMS-98}$, while in several town blocks and districts it approached IX_{EMS-98}.

B2. Mianzhu Town. The town of Mianzhu is located 80 km northeast of the town of Dujiangyan and only 10 km southeast of the surface fault rupture. It is estimated that 20% of the buildings totally or partially collapsed, while 60% of the buildings suffered considerable damage. Mostly multistory buildings, both modern and older, were damaged, while single or double-story constructions suffered less. Dominant causes for the damage in many constructions were the architectural peculiarities and features, especially in cases of constructions with frames lacking proper seismic design. Moreover, many schools, hospitals, and industrial units collapsed, causing thousands of casualties while the infrastructure was either destroyed or seriously damaged (Fig. 7). The town expands practically on the foothills of the mountainous region to the west, while the foundation formations are alluvial deposits and debris that mainly develop toward the east.

The estimated intensity in the area exceeded $VIII_{EMS-98}$ and locally approached IX_{EMS-98}.

B3. Anxian Town. The town of Anxian is located 120 km northeast of the town of Dujiangyan and only 5 km southeast of the seismic fault. It is estimated that 30% of the buildings totally or partially collapsed, while 50% of the buildings suffered considerable damage. Again, the high buildings (more than three stories high) were affected. A significant number of schools, hospitals, and industrial units collapsed, causing thousands of casualties, while the infrastructure was either destroyed or seriously damaged. The estimated intensity in the area exceeded IX_{EMS-98} and locally approached X_{EMS-98}.

Figure 6. A building in Dujiangyan founded on river deposits with serious structural damage on the ground floor props (type of construction D, damage degree 4). The color version of this figure is available only in the electronic edition.

Area C

Area C, which corresponds to the hanging wall of the fault, is the mountainous part of the Tibetan Plateau. Damage in this area was widespread to a distance of approximately 100 km northwest (Fig. 2, 3).

C1. The Beichuan Regions. The Beichuan, Yingxiu, Dujiangyan (Guanxian), and Jiangyou towns, as well as smaller settlements, are scattered in the mountainous western section of the affected region. They are located mainly on flat areas and especially on older and modern river terraces, usually straddling the rivers; for instance, the Min River runs through Yingxiu and Guanxian, and the Jian River runs through Beichuan. Both slopes and river terraces are composed of unconsolidated formations and more specifically

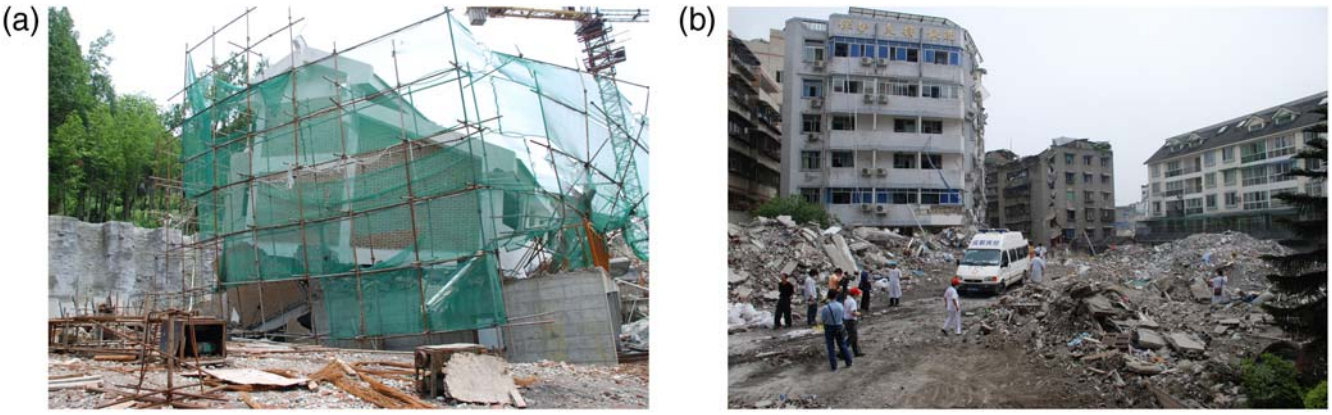

Figure 5. (a) A recently constructed building at the suburbs of Dujiangyan that collapsed (type of construction D, damage degree 5) and (b) a hospital unit in the same town that totally collapsed (type of construction D, damage degree 5). The color version of this figure is available only in the electronic edition.

Figure 7. (a) Buildings in Mianzhu town that suffered severe damage. Buildings with partial or total collapse could be seen (type of construction D, damage degree 5) and (b) buildings that suffered minor or no structural damage (type of construction D, damage degree 3). The color version of this figure is available only in the electronic edition.

by river—stream deposits characterized by the predominance of pebbles, conglomerates, and poorly graded material and by recent and older debris, as well as fans of variable thickness. These formations cover most of the Tibetan Plateau.

The trace of the main branch of the seismic fault (Yingxiu–Beichuan fault) leaves an impressive imprint on the topography from the suburbs of the Beichuan and Yingxiu towns, and it can be followed throughout the rest of the area, including the smaller towns. Collapses were highly localized in a 150-m-wide zone on either side of the fault trace.

All damage recorded in old and new constructions resulted from the aforementioned morphological, geological, tectonic, and geotechnical setting. In the Wenchuan region, 85% of the constructions collapsed partially or totally, while the rest suffered significant structural damage. It is indicative that only a few buildings (< 15%) did not suffer partial or total collapse. Furthermore, the infrastructures suffered considerable damage within and beyond the urban center, with a general failure of bridges and road network (Lin *et al.*, 2008). In addition, large-scale landslides were triggered in many places, completing the picture of devastation (Fig. 8).

An unusual behavior was exhibited by the existing dams in the mountainous region. More specifically, according to official data, 300 out of 450 dams in the region suffered considerable damage, while some caused serious problems downstream due to the excessive water flow. In a great number of dams, the crown was destroyed and the connection between the two sides of the dam was not possible, blocking the road network for a considerable number of areas. It is estimated that 30% of the dams in the mountainous region

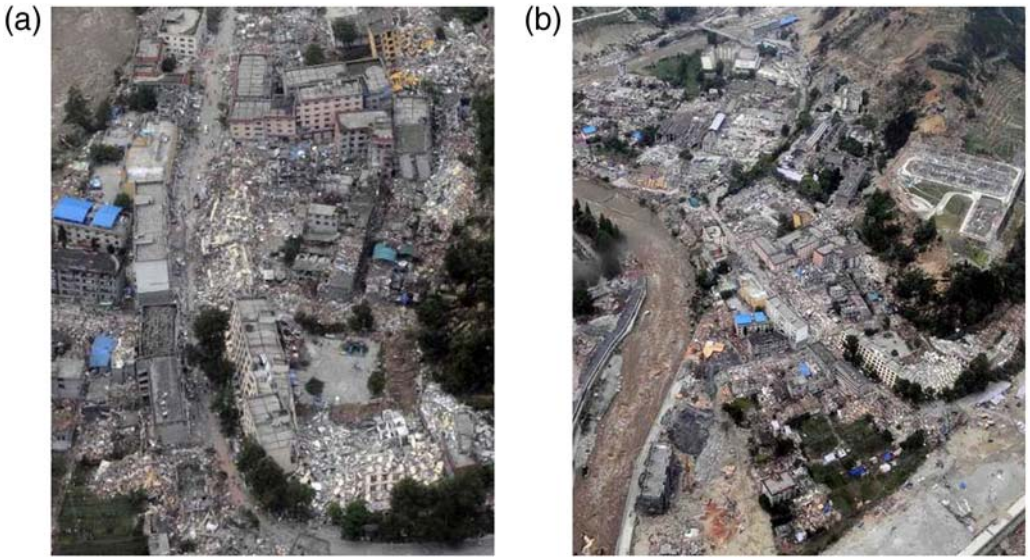

Figure 8. Oblique aerial view of residential constructions in the Beichuan and Yingxiu towns that suffered total destruction. These towns were founded on river terraces in the mountainous region. Large-scale landslides on the surrounding slopes contributed to the destruction of the residential constructions [(a) Photo courtesy of British Broadcasting Corporation, 2008; (b) photo courtesy of Reuters, 2008]. The color version of this figure is available only in the electronic edition.

have been completely destroyed, and their restoration is not feasible. The estimated maximum intensity for this region is $XI_{EMS\text{-}98}$, while in some locations (e.g., Beichuan and Yingxiu towns) approached $XII_{EMS\text{-}98}$.

C2. Wenchuan Town–Maoxian Town. The towns of Wenchuan and Maoxian are located 30 km west of the activated Yingxiu–Beichuan fault branch, along the Wenchuan–Maoxian fault branch that was not activated during the earthquake.

Both towns and smaller settlements in the area are characterized by the same morphological, geological, and geotechnical setting that was described earlier, involving steep morphology, complex geological structure, and unfavorable geotechnical conditions.

In all settlements, buildings collapsed or suffered considerable structural damage to an extent that exceeded 50%. It is indicative that only a small percentage of the constructions (not more than 20%) was left intact. In addition, infrastructures such as bridges, tunnels, and dams either collapsed or suffered considerable damage. Finally, in the greater region, landslides and rockfalls were recorded due to the high energy relief and the unconsolidated lithologies that caused additional damage in settlements and infrastructure.

The general estimated intensity for this region reached $X_{EMS\text{-}98}$.

Intensity Estimation According to ESI 2007

Extended observations and recordings were carried out in the study area to investigate the primary and secondary effects based on the ESI 2007 guidelines (Michetti *et al.*, 2007). The new Environmental Seismic Intensity Scale (ESI 2007), introduced by the International Union for Quaternary Research (Michetti *et al.*, 2007), incorporates the advances and achievements of [alaeoseismology and earthquake geology and evaluates earthquake size and epicenter solely from the earthquake environmental effects (EEE; Michetti *et al.*, 2007; Lalinde and Sanchez, 2007; Ali *et al.*, 2009). Traditional intensities describe the effects on human parameters. However, when using the effects on man and the man-made environment to assess the macroseismic intensity, the intensity will tend to reflect mainly the economic development and the cultural setting of the area that experienced the earthquake, instead of its so-called strength (Serva, 1994). The ESI 2007 tries to cover this weakness, and its use may reduce the uncertainties implied in intensity attenuation laws worldwide, assisting seismic hazard studies (Papanikolaou *et al.*, 2009).

Observations of the primary and secondary effects were carried out in a region exceeding 50,000 km^2 and are presented for each area from west to east in the following sections. Recent publication data were taken into account (Chen *et al.* 2008; EERI, 2008; Hao *et al.*, 2008; Lekkas, 2008a; Lekkas 2008b; Li *et al.* 2008; Zhao *et al.*, 2008). The main results are summarized in Table 1.

Area A

A1. Significant variations of the water level in wells and the discharge rates of springs, as well as small variations of the physical properties of water, were locally recorded; turbidity in lakes, springs, and wells were also observed.

A2. Fractures up to 5–10 cm wide and up to a 100 m long were observed, commonly in loose alluvial deposits and saturated soils. Centimeter-wide cracks were common in paved asphalt roads.

A3. Liquefaction was frequently recorded in the area, depending on local conditions. The most typical effects were: sand boils up to 1 m in diameter; apparent water fountains in still waters; localized lateral spreading and settlements (subsidence up to 30 cm), with fissuring parallel to waterfront areas (river banks, lakes, canals) (Chen *et al.*, 2008). The main features of the liquefied sites are: (1) liquefaction of soil in low intensity regions (e.g., regions of seismic intensity of VI) and of some medium-grained and fine-grained sands, and (2) destructions were often caused by the liquefaction rather than ground shaking (Chen *et al.*, 2008).

The overall estimated intensity value for Area A is $VII–VIII_{ESI\ 2007}$.

Area B

B1. Ground ruptures up to a few kilometers long were recorded, with offsets generally in the order of several centimeters.

B2. Springs changed their flow-rate, generally temporarily. Some modest springs even ran dry. Temporary variations of water level were also observed in wells. Variations of chemical–physical properties of water, most commonly temperature, were observed in springs. Water turbidity was common in closed basins, rivers, wells, and springs.

B3. Fractures up to 100 cm wide and up to hundreds of meters long were observed in loose alluvial deposits and saturated soils. Cracks and small pressure undulations were common in paved asphalt roads.

B4. Landslides were widespread in prone areas and on gentle slopes, as well as rockfalls on steep gorges, their size being frequently large (10^5 m^3). Landslides blocked many valleys, preventing water runoff and thus producing temporary or even permanent small lakes. Many riverbanks, artificial embankments, and excavations also collapsed.

B5. Liquefaction and water upsurges were frequent; sand boils up to 3 m in diameter are present. The most typical effects were: apparent water fountains in still waters and frequent lateral spreading and settlements (subsidence of more than 30 cm), with fissuring parallel to waterfront areas.

Table 1

Conclusive Remarks from Field Data According to ESI 2007*

		Primary Effects					Secondary Effects		
		Surface Faulting and Deformations	Hydrological Anomalies	Anomalous Waves/Tsunamis	Ground Cracks	Slope Movement	Liquefactions	Jumping Stones	Total Area
VI	SLIGHTLY DAMAGING; Modest effects in the environment								
VII	DAMAGING; Appreciable effects in the environment		A1		A2				
VIII	HEAVILY DAMAGING; Extensive effects in the environment						A3		10 km^2
IX	DESTRUCTIVE; Effects in the environment are a widespread source of considerable hazard and become important for intensity assessment	B1	B2		B3	B4	B5	B6	1000 km^2
X	VERY DESTRUCTIVE; Effects in the environment become a leading source of hazards and are critical for intensity assessment						C6		5000 km^2
XI	DEVASTATING; Effects in the environment become decisive for intensity assessment, due to saturation of structural damage		C2	C3	C4	C5		C7	10,000 km^2
XII	COMPLETELY DEVASTATING; Effects in the environment are the only tool for intensity assessment	C1							50,000 km^2

*Column entries refer to specific subsections of intensity estimation according to ESI 2007.

Figure 9. The artificial lake that was formed along the course of the Min River by the Zipingpu Dam. During the earthquake, large-scale landslides (background) triggered water waves 15 m high. The color version of this figure is available only in the electronic edition.

B6. Small boulders and tree trunks were thrown in the air and carried meters away from their site, depending on slope angle and roundness, leaving typical imprints in soft soil.

The estimated intensity value for area B is $IX_{ESI2007}$

Area C

C1. As reported earlier in this paper, this earthquake generated a 220-km surface rupture along the Yingxiu–Beichuan fault and a 72-km surface rupture along the Guanxian–Anxian fault. Maximum vertical and horizontal displacements of 6.2 m and 4.9 m, respectively, were observed along the Yingxiu–Beichuan fault, whereas a maximum vertical and horizontal displacement of 3.5 m and 1.0 m, respectively, occurred along the Guanxian–Anxian fault (Chen *et al.*, 2008; Hao *et al.*, 2008; Xu *et al.*, 2008). Drainage lines presented a significant offset, obstructing water flow. These large primary effects clearly affected and modified the topography of the area.

C2. Many springs significantly changed their discharge rates and outcrop localities. Additionally, many springs ran temporarily or even permanently dry. Temporary or permanent variations of water level were observed in wells. Strong variations of physical properties of water, most commonly temperature, was observed in springs. Water became very muddy in large basins, rivers, wells, and springs.

C3. Intense water undulations were recorded in the lakes of the area either due to the earthquake tremor or due to landslides triggered at the banks. It is worth mentioning that, in the artificial lake of the Zipingpu dam, extensive landslides in the surrounding mountains generated waves that exceeded 10 meters in height, causing the deaths of approximately 100 fishermen (Fig. 9).

C4. Open ground cracks up to several meters wide were frequently recorded, mainly in loose alluvial deposits. In competent rocks, they did not exceed 1 m. Very wide cracks and large pressure undulations developed in paved asphalt roads.

C5. Large landslides and rock-falls ($> 10^5$–10^6 m^3) were frequently recorded, practically regardless of equilibrium state of slopes (Fig. 10, Fig. 11, and Fig. 12), producing many temporary or permanent barrier lakes. River banks, artificial embankments, and sides of excavations collapsed. Levees and earth dams incurred serious damage (Lekkas, 2008b; Zhao *et al.*, 2008; Xu *et al.*, 2009).

C6. Liquefaction, with water upsurge and soil compaction, was recorded that changed the aspect of wide zones; sand volcanoes more than 8 m in diameter, vertical subsidence >3 m, and large and long fissures due to lateral spreading were common.

C7. Massive boulders, several meters in diameter, were thrown up in the air and rolled away from their original location for long distances, even at gentle slopes.

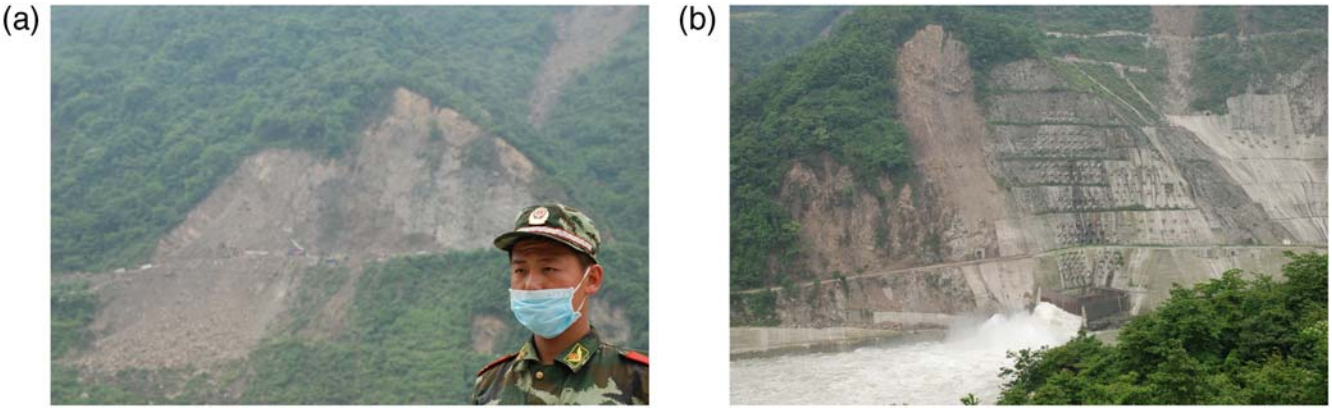

Figure 10. (a) Large-scale landslides that were triggered in the mountainous region along river Min. (b) The Zipingpu Dam. The color version of this figure is available only in the electronic edition.

Figure 11. Partial view of Beichuan town, which was almost totally destroyed (ESI 2007 = XII) due to the combined action of the seismic fault Yingxiu–Beichuan (arrows) and the massive landslides. The color version of this figure is available only in the electronic edition.

The estimated intensity values for area C range from X to $XII_{ESI2007}$.

Discussion and Conclusions

The earthquake of 12 May 2008 in Sichuan county, China, can be classified as a large-scale event, based on the size of the tectonic structures that were activated during the earthquake and the effects caused on the human and natural environment.

Macroseismic intensity values could be estimated for a broad area around the epicenter based on the EMS-98 and the ESI 2007 scales (Figs. 13–16).

Figure 12. Partial view of Beichuan town, which was totally destroyed by the earthquake and a huge landslide. The color version of this figure is available only in the electronic edition.

Area A is characterized by intensities $VI–VII_{EMS-98}$. The low-intensity recordings are due to the flat relief, the relatively favorable geotechnical conditions, and their location on the footwall and, more precisely, away from the activated fault zone. As a result, damage in buildings was limited, generally decreasing toward the east-southeast, as the horizontal distance from the seismic fault increased. In the area, the recorded values of $VII–VIII_{ESI\ 2007}$ (compared to $VI–VII_{EMS-98}$) are locally higher by one degree, owing mainly to the widespread liquefactions, hydrological changes, and ground failure. These phenomena were favored by the existing morphological, hydrogeological, and geotechnical setting of the Sichuan basin region, which exhibits a dense river network with minor and major rivers and streams and a shallow water table. These areas are not characterized by urban development. Nevertheless, there is a general agreement in the intensity values of both the EMS-98 and the ESI 2007 for area A.

Area B corresponds to the intermediate morphological zone between the high relief of the Tibetan Plateau to the northwest and the Sichuan basin to the southeast bounded toward the northwest by the trace of the seismic fault. It is characterized by a complex relief crossed by a dense river network, alluvial deposits, and debris fans. There, the values according to the EMS-98 reached VIII and only locally approached IX, while the values according to the ESI 2007 reached IX. The highly developed drainage network, the shallow water table, the unconsolidated, partly cohesive material of the alluvial deposits, and the intense phenomena of erosion and deposition of unconsolidated material compose a weak geotechnical setting for the development of urban centers. These factors favored the triggering of secondary gravitational phenomena and the intense morphological changes that directly affected the values of the ESI 2007. Area B experienced stronger damage and larger and more diffuse EEE because, despite its location on the footwall of the activated fault, it was very close to the rupture zone.

Area C corresponds to the portion of the Tibetan Plateau characterized by high relief, steep slopes, a dense river network, deep incisions, and intense erosion. It incorporates the tectonic structure that was activated during the earthquake and develops toward the west, corresponding to the causative fault hanging wall. In area C, the EMS-98 and ESI 2007 intensity values are generally in agreement. The values $X–XII_{EMS-98}$ represent extended collapses of constructions due to the unfavorable geotechnical and geomorphological conditions. The values of $X–XII_{ESI\ 2007}$ derive from the extensive primary surface ruptures and the secondary effects (such as ground ruptures, large-scale landslides, and tsunamis in lakes) that developed in numerous places, extending in a large area as a result of the geomorphological conditions. The ESI 2007 provides a reliable estimation of earthquake size with increasing accuracy toward the highest levels of the scale, where traditional scales saturate and ground effects are the only ones that permit a reliable estimation of earthquake size (Michetti *et al.*, 2004). In Wenchuan, the extensive spatial distribution of damage and the relatively poor quality

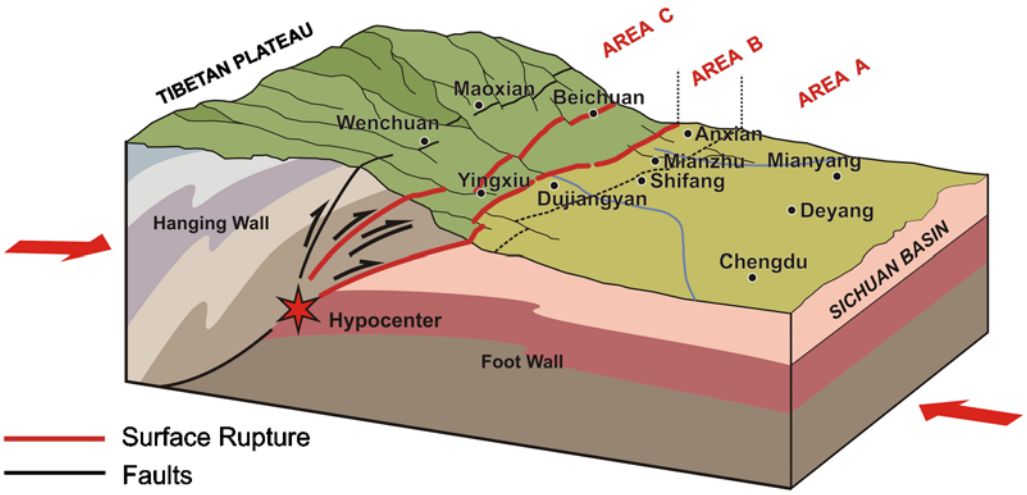

Figure 13. Location of the activated faults and the areas A, B, and C that were characterized by different intensity values. The color version of this figure is available only in the electronic edition.

of the buildings do not permit accurate evaluation of intensities higher than X, due to saturation effects. On the other hand, the EEE provide a clear and more accurate view of the intensities in the epicentral area.

The application of both EMS-98 and ESI 2007 and the comparison of the results based on the geodynamic, seismotectonic, geomorphological, and geotechnical setting of the region affected by the 12 May 2008 earthquake suggest the following conclusions (Fig. 15 and 16):

1. No significant variations on the values of both intensity scales were recorded during their application for the areas A, B, and C, which correspond to three clearly distinct areas: (a) the flat lowland area of the Sichuan basin, located southeast of the trace of the seismic fault, (b) the elongated zone of a general northeast—southwest direction with complex topography, located to the southeast of the seismic fault trace, and (c) the region that includes the occurrence of extensive surface faulting to the west and corresponds to the Tibetan Plateau.
2. Approximately 2–4 degrees of difference in the intensity values were recorded between the footwall (area A) and the hanging wall (area C). In area B, to the southeast of the activated fault zone, intermediate values were estimated.
3. Despite the fact that the general EMS-98 and ESI 2007 estimates for each area (A, B, and C) were almost in

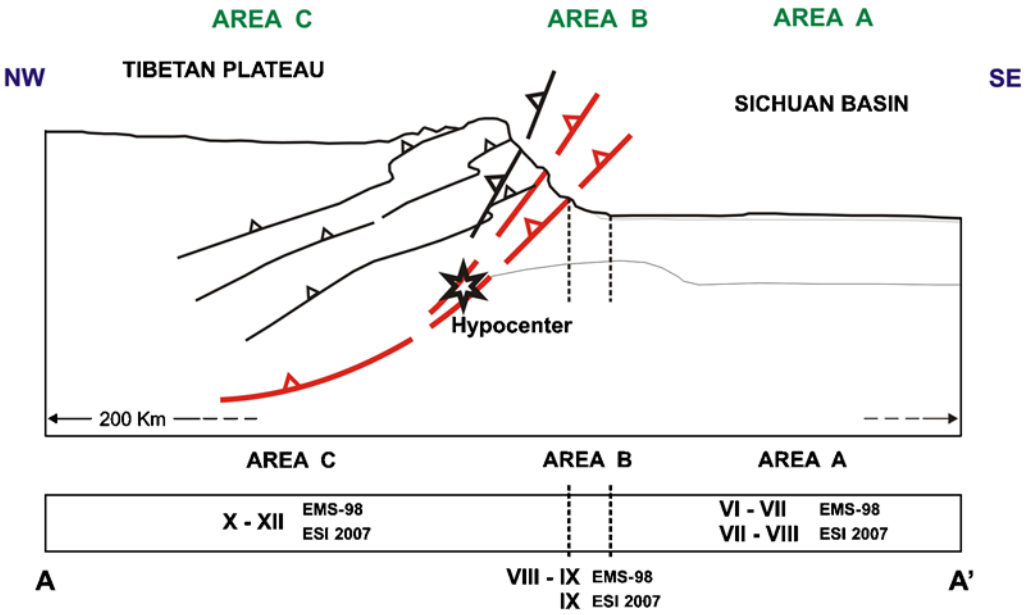

Figure 14. Northwest–southeast-trending cross section with the locations of areas A, B, and C and the estimated values according to EMS-98 and ESI 2007 intensity scales. The color version of this figure is available only in the electronic edition.

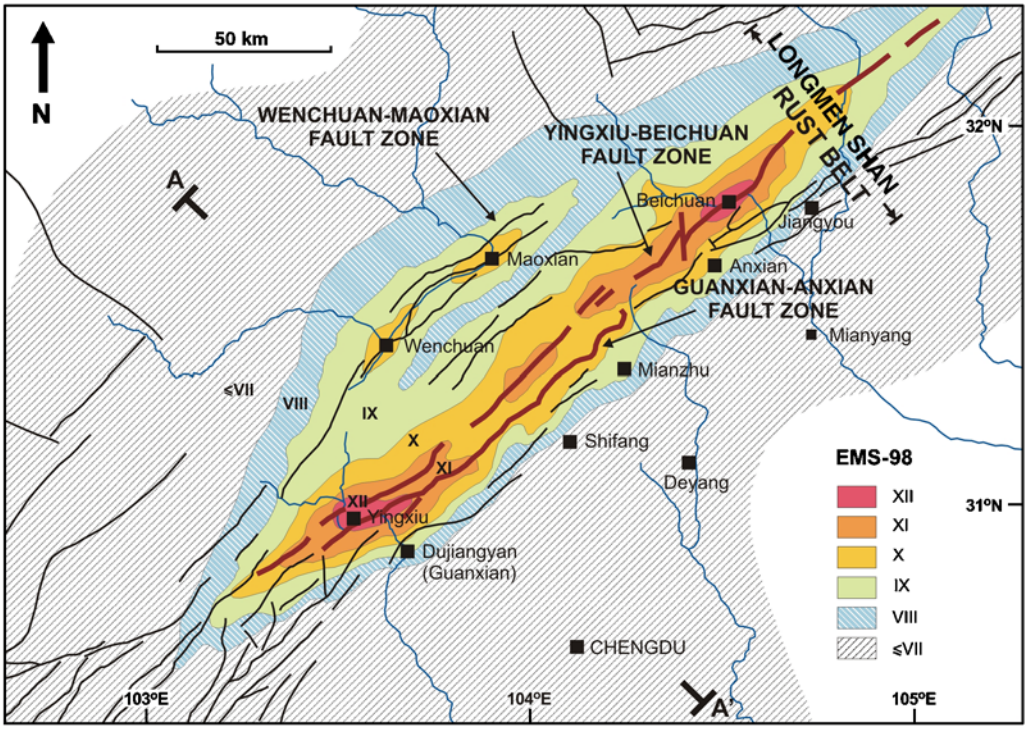

Figure 15. EMS-98 intensity distribution map of the meisoseismal area. The color version of this figure is available only in the electronic edition.

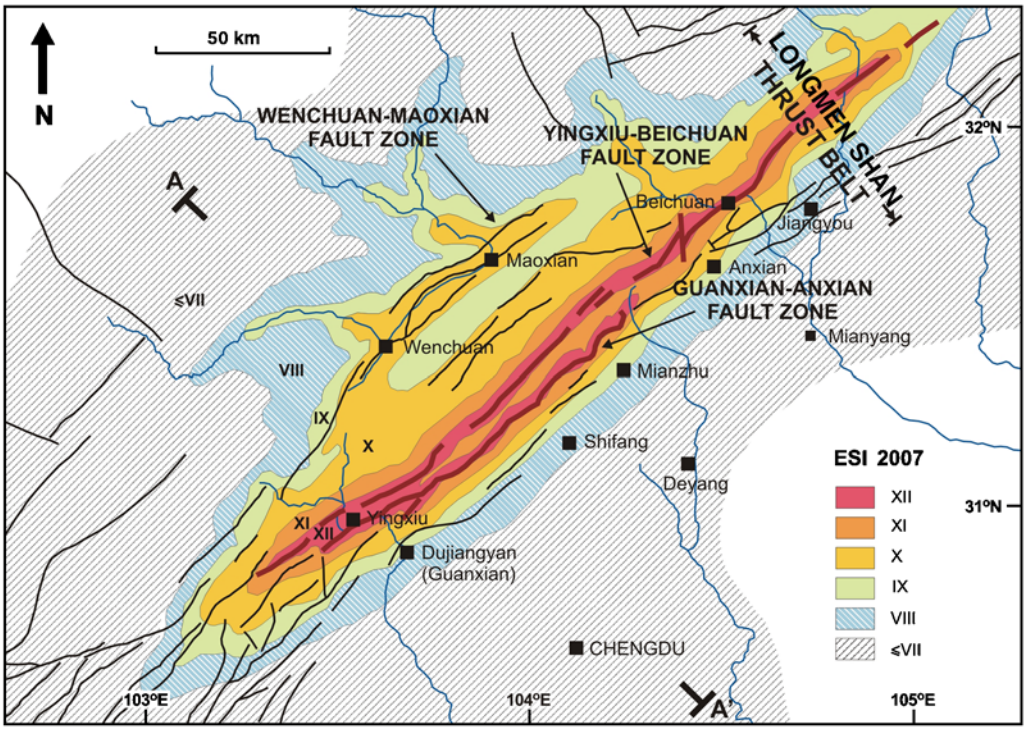

Figure 16. ESI 2007 intensity distribution map of the meisoseismal area. The color version of this figure is available only in the electronic edition.

agreement, the geographical distribution of the assessed sites was different. This result corroborates the validity of the ESI scale and its value to obtain a more complete and reliable picture of intensity distribution, especially for high intensities and less urbanized areas, which is actually its main objective (Michetti *et al.*, 2007).

Thus, the application and use of both EMS-98 and ESI 2007 represents a fundamental tool for the estimation of seismic hazard in a region and should be encouraged. In particular, the ESI 2007 could be applied to past, even prehistoric, events because it is based on geological effects rather than being biased by cultural/technical differences, either in time or space.

Data and Resources

All data used in this paper came from the published sources listed in the references.

Acknowledgments

The author would like to thank the reviewers and special-issue guest editor Yann Klinger for their helpful suggestions and comments.

References

Ali, Z., M. Qaisar, T. Mahmood, M. A. Shah, T. Iqbal, L. Serva, A. M. Michetti, and P. W. Burton (2009). The Muzzaffarabad, Pakistan, earthquake of 8 October 2005: Surface faulting, environmental effects and macroseismic intensity, *Spec. Publ. Geol. Soc. Lond.* **316,** 155–172.

Burchfiel, B. C. (2004). New technology, new geological challenges, *GSA Today* **14,** no. 2, 4–7.

Burchfiel, B. C., Z. Chen, Y. Liu, and L. H. Royden (1995). Tectonics of the Longmen Shan and adjacent regions, central China, *Int. Geol. Rev.*, **37,** 661–738.

Burchfiel, B. C., L. H. Royden, R. D. van der Hilst, and B. H. Hager (2008). A geological and geophysical context for the Wenchuan earthquake of 12 May 2008, Sichuan, People's Republic of China, *GSA Today* **18,** no. 7, 4–11.

Chen, L., L. Hou, Z. Cao, X. Yuan, R. Sun, W. Wang, F. Mang, H. Chen, and L. Dong (2008). Liquefaction investigation of Wenchuan earthquake, paper no. S31-049*14th World Conf. on Earthquake Engineering*, Beijing, China, 12–17 October 2008.

Densmore, A. L., M. A. Ellis, Y. Li, R. Zhou, G. S. Hancock, and N. Richardson (2007). Active tectonics of the Beichuan and Pengguan faults at the eastern margin of the Tibetan Plateau, *Tectonics* **26,** TC4005, doi 10.1029/2006TC001987.

Earthquake Engineering Research Institute (EERI) (2008). The Wenchuan, Sichuan Province, China, earthquake of May 12, 2008, *EERI Special Earthquake Report, October 2008*, Oakland, California, 12 pp.

Gan, W. J., P. Z. Zhang, Z. K. Shen, Z. J. Niu, M. Wang, Y. G. Wan, D. M. Zhou, and J. Cheng (2007). Present-day crustal motion within the Tibetan Plateau inferred from GPS measurements, *J. Geophys. Res.* **112,** B08416, doi 10.1029/2005JB004120.

Grünthal, G. (Editor). (1998). European Macroseismic Scale 1998, *Conseil de l' Europe* **15,** 99.

Hao, K. X. S., H. Si, and H. Fujiwara (2008). A preliminary investigation of the coseismic surface-ruptures for Wenchuan earthquake of 12 May 2008, Sichuan, China, paper no. S31-007, *14th World Conf. on Earthquake Engineering*, Beijing, China, 12–17 October 2008.

Houssam, M. A., Y. Li, A. S. Oday, A. A'ssim, and L. Wang (2008). A comprehensive analysis of the devastating Wenchuan earthquake of May 12th 2008, paper no. S31-014, *14th World Conf. on Earthquake Engineering*, Beijing, China, 12–17 October 2008.

Hu, J. J., L. L. Xie, and J. W. Dai (2008). Characteristics of engineering damage and human mortality in Mianzhu areas in the great 2008 Wenchuan, Sichuan, earthquake, paper no. S31-024, *14th World Conf. on Earthquake Engineering*, Beijing, China, 12–17 October 2008.

Hubbard, J., and J. Shaw (2009). Uplift of the Longmen Shan and Tibetan Plateau, and the 2008 Wenchuan (M = 7.9), *Nature* **458,** 194–197.

Kabeyasawa, T., T. Kabeyasawa, K. Kusunoki, and K. Li (2008). An outline of damages to school buildings in Dujiangyan by the Wenchuan earthquake on May 12, 2008, paper no. S31-002, *14th World Conf. on Earthquake Engineering*, Beijing, China, 12–17 October 2008.

Lalinde, C.-P., and J. J. Sanchez (2007). Earthquake environmental effects in Colombia during the past 35 years: INQUA Scale Project, *Bull. Seismol. Soc. Am.* **97,** 646–654.

Lekkas, E. (2008a). Wenchuan earthquake (M_w 7.9, 12 May 2008) Sichuan, China. Geotectonic regime and damage macro-distribution, paper no. S31-015, *14th World Conf. on Earthquake Engineering*, Beijing, China, 12–17 October 2008.

Lekkas, E. (2008b). Zipingpu Dam failures (Sichuan Prefecture, China) caused by the 7.9R earthquake on the 12th May 2008, *ESC 2008, 31st General Assembly*, Hersonissos, Crete, 238–239.

Li, X., Z. Zhou, M. Huang, R. Wen, H. Yu, D. Lu, Y. Zhou, and J. Cu (2008). Introduction and preliminary analysis of strong motion recordings from the 12 May 2005 Ms 8.0 Wenchuan earthquake Of China, paper no. S31-052, *14th World Conf. on Earthquake Engineering*, Beijing, China, 12–17 October 2008.

Lin, J. C. C., H. H. Hung, K. Y. Liu, and J. F. Chai (2008). Reconnaissance report of 0512 China Wenchuan earthquake on bridges, paper no. S31-006, *14th World Conf. on Earthquake Engineering*, Beijing, China, 12–17 October 2008.

Lu, J., Z. K. Shen, and M. Wang (2003). Contemporary crustal deformation and active tectonic block model of the Sichuan-Yunnan region, China, *Seismol. Geol.* **25,** no. 4, 543–554.

Massachusetts Institute of Technology (2008). Earthquake near Wenchuan, West Sichuan, China 2008 May 12 06:28:01 UTC; Magnitude 7.9, http://quake.mit.edu/~changli/wenchuan.html (last accessed September 2008).

Michetti, A. M., E. Esposito, L. Guerrieri, S. Porfido, L. Serva, R. Tatevossian, E. Vittori, F. Audemard, T. Azuma, J. Clague, V. Comerci, A. Gürpinar, J. Mccalpin, B. Mohammadioun, N. A. Mörner, Y. Ota, and E. Roghozin (2007). Environmental Seismic Intensity Scale 2007—ESI 2007, in *Memorie Descrittive della Carta Geologica d'Italia, 74, 7-54*, L. Guerrieri and E. Vittori (Editors), Servizio Geologico d'Italia—Dipartimento Difesa del Suolo, APAT, Roma, Italy, 1–41.

Michetti, A. M., E. Esposito, A. Gurpinar, B. Mohammadioun, J. Mohammadioun, S. Porfido, E. Rogozhin, L. Serva, R. Tatevossian, E. Vittori, F. Audemard, V. Comerci, S. Marco, J. McCaplin, and N. A. Morner (2004). The INQUA scale: An innovative approach for assessing earthquake intensities based on seismically-induced ground effects in natural environment, *Spec. Pap. Mem. Descr. Carta Geologica D' Italia LXVII*, APAT, Rome, Italy, 118 pp.

Papanikolaou, I. D., D. I Papanikolaou, and E. L. Lekkas (2009). Advances and limitations of the environmental seismic intensity scale (ESI 2007) regarding near-field and far-field effects from recent earthquakes in Greece: Implications for the seismic hazard assessment, in *Paleoseismology: Historical and Prehistorical Records of Earthquake Ground Effects for Seismic Hazard Assessment*, Special Publication 316 of the Geological Society of London, K. Reicherter, A. M. Michetti, and P. G. Silva (Editors), Geological Society of London, London, 11–30.

Royden, L. H., B. C. Burchfiel, and R. D. van der Hilst (2008). The geological evolution of the Tibetan Plateau, *Science* **321,** no. 5892, 1054–1058.

Serva, L. (1994). Ground effects in the intensity scales, *Terra Nova* **6,** 414–416.

Sun, J., Q. Meng, Q. Ma, H. Shi, and Z. Sun (2008). Outline introduction of building damage in high intensity areas of Wenchuan *M* 8.0 earthquake, paper no. S31-020, *14th World Conf. Earthquake Engineering*, Beijing, China, 12–17 October 2008.

Tectonics Observatory of Caltech (2008). *The science behind China's 2008 Sichuan earthquake*, http://www.tectonics.caltech.edu/outreach/highlights/2008MayChinaEQ/index.html (last accessed May 2008).

U.S. Geological Survey (USGS) (2008). *Magnitude 7.9—Eastern Sichuan, China* http://earthquake.usgs.gov/eqcenter/eqinthenews/2008/us2008ryan/ (last accessed June 2008).

Xu, Q., X. M. Fan, and C. V. Westen (2009). Landslide dams triggered by the Wenchuan earthquake, Sichuan Province, south west China, *Bull. Eng. Geol. Environ.* **68,** no. 3, 373–386.

Xu, G., W. Fang, P. Shi, and Y. Yuan (2008). Fast assessment on residential building loss and population displacement after the great Wenchuan earthquake disaster, paper no. S31-041, *14th World Conf. on Earthquake Engineering*, Beijing, China, 12–17 October 2008.

Zhang, P. Z., Z. Shen, M. Wang, W. J. Gan, R. Burgmann, and P. Molnar (2004). Continuous deformation of the Tibetan Plateau from global positioning system data, *Geology* **32,** 809–812.

Zhao, J., Z. Zhou, and J. Wu (2008). Investigation of landslide and rockfall caused by Wenchuan earthquake of M_s 8.0, paper no. S31-050, *14th World Conf. on Earthquake Engineering*, Beijing, China, 12–17 October 2008.

Professor of Dynamic Tectonic Applied Geology
Faculty of Geology and Geoenvironment
University of Athens
Panepistimioupoli Zografou
Athens 15784, Greece
elekkas@geol.uoa.gr

Manuscript received 31 August 2009